Voltage stability enhancement Scheme using PV-reinforced Dynamic Voltage Restorer

J. A. Joseph, G. A. Olarinoye, A. S. Abubakar
Department of Electrical Engineering, Ahmadu Bello University, Zaria–Nigeria. jajoseph@gmail.com *(Corresponding Author)*

Keywords: –
Dynamic Voltage Restorer;
Photovoltaic;
Harmonic Reduction;
voltage sags;
Faults.

Article History: –
Received:. July 14, 2023
Reviewed: Sept. 22, 2023
Accepted: Nov. 13, 2023
Published: Dec. 28, 2023

ABSTRACT

Among the promising solutions proposed for the mitigation of the voltage instabilities is a series compensator known as Dynamic Voltage Restorers (DVR) due to its flexibility and cost effectiveness. Dynamic Voltage Restorer (DVR) also known as Static Synchronous Series Compensator (SSSC) is a series compensation technique used in the distribution and transmission system. The power flow through the supply line is regulated by controlling the equivalent impedance of the line. The output voltage of DVR is fully controlled and independent of the line current In conventional DVR, capacitors or supercapacitors are used at the DC-link as energy storage elements. However, due to the self-discharge rate and gradual voltage loss of capacitors and supercapacitors, the stored voltage drops linearly as the capacitor is discharging, thereby making the DVR not suitable for voltage stabilization following a prolonged disturbance. In this study, the DC-link of conventional DVR is reinforced with Photovoltaic (PV) and battery with aim to mitigate the devastating impact of symmetrical and unsymmetrical faults on the load voltage. Specifically, the PV-reinforced DVR is developed to mitigate voltage sags(and harmonics) caused by three phase symmetrical fault as well as unsymmetrical faults. In order to mitigate the harmonics generated due to the injection of compensation voltage, a filter is implemented to lessen the effect. To verify the performance of the developed PV-reinforced DVR, the system is designed in MATLAB/Simulink where a time-based simulation is carried out. It is established that the PV reinforcement to the DC-link has significantly improved the DVR response to the voltage sag at the PCC. Similarly, the filter designed has led to remarkable reduction in the THD. For the three phase fault, the load voltage is improved from the faulted condition of 20.18V to 319.36V by injecting a three phase voltage of 298.24V. The load voltage of 298.24V obtained represents 22.56% improvement on the voltage of 260.5V obtained using the technique of PID-DVR. For the DLG fault, the phase voltages are improved from faulted condition of 126.4V to 323.66V in both phases, which represents 12.77% improvement over those obtained using PID-DVR. The Total Harmonic Distortion obtained using PV-reinforced DVR in the two scenarios were reduced from 3.64% to 2.84% (21.98% reduction), 5.10% to 3.96% (22.35% reduction) for the three phase, double line-to-ground faults scenarios respectively.

1. INTRODUCTION

Due to the massive expansion in industrial activities, technological advancement and stringent requirement to supply a qualitative power, the effort to improve the quality of electrical power have significantly increased (Abdelkader, *et al.*, 2022). Introduction of sophisticated equipment for wide range of applications have made the quality of electrical power more essential. Power Quality (PQ) is concerned with characteristics of electrical power supply delivered under normal operation conditions that do not interrupt customer's process. Poor power quality creates a number of problems ranges from equipment mal-function, which result to overheating of rotating machinery, random tripping of relays for protection of devices. PQ is a broad term that covers many issues concerning electrical supply interruptions or fluctuations (Callegari, *et al.*, 2021).

Typical power quality issues include transients, flickers, voltage sags, swells, phase imbalances, frequency deviations and other distortions to the sinusoidal waveform due to the harmonics

(AlMathnani, *et al*., 2021). Some of these problems are sustained momentarily while others like the harmonics represent a steady-state problem, for as long as the harmonic generating equipment in the system is in operation. One of the most essential power quality issues is voltage sag which contributes to about 90% of the problems. The major causes of voltage sag are (Dehnavi, *et al.*, 2022):2

i. Short circuits,
ii. Large motor starting,
iii. The high inrush current in transformers,
iv. Sudden load changes,
v. Energizing transformer, depending on the transformer connections,

A voltage sag can cause relays and contactors in motor starters (adjustable speed drives), process controllers to fail, since they are more sensitive to voltage sags (Berbaoui & Brahim, 2017; Boonchiam & Mithulananthan, 2006).

Moreover, a three-phase system can be subjected to major degree of imbalance because of the presence of single-phase loads and/or distributed generations (DGs) units (Callegari, *et al*., 2021; Farooqi, *et al*., 2022). Dynamic voltage restorer has been used to avert this.

Moreover, in spite of the improvements by various research works on the operation of DVR, very few addressed the limitation of the storage capacity of the DC-link. The capacitor at the DC-link of DVR can be drained if there is prolonged voltage sagging, thereby making it inapt for voltage stabilization for a prolonged disturbance (Boonchiam & Mithulananthan, 2006). As such, this study proposed reinforcing the DC-link capacitor with a battery and a PV system. Envisioned that strengthening the DC-link energy storage, the DVR can mitigate the devastating impact of unsymmetrical faults and sudden load variations for longer time by injection of series compensating voltages devoid of draining the DC-link capacitor. Similar attempt was made in (Prasad & Dhanamjayulu, 2022), where a solar PV integrated DVR with aid of a rotating d-q reference frame controller to improve power quality issues. However, the study focused on the enhancement of the PV's Maximum Power Point Tracking (MPPT) controller using Adaptive Neuro-Fuzzy Inference System. While improving the MPPT of the PV system, little or no attention was paid to its overall impact of the DVR's DC-link and harmonic current injection to the system (Shakir & Sharma, 2019; Rao, *et al*., 2015).

Therefore, the PV-reinforced DVR is designed to mitigate voltage sags initiated by unsymmetrical faults. For the suppression of the harmonics generated by the the injection of compensation voltage from the DVR, a filter is designed to lessen the harmonic effect. The voltage disturbances coming either from the supply or load side is mitigated at the Point of Common Coupling (PCC). The system is simulated in MATLAB/Simulink where a time-based simulation is carried out. The results are validated using IEEE519 standards and a comparative analysis with a similar study using voltage sags and %THD as performance metrics.

2. PV-REINFORCED DVR SYSTEM DESIGN

The developed DVR is reinforced via the DC-link with aid of Photovoltaic (PV) and battery so as to mitigate devastating impact of bolted three phase and unsymmetrical faults on the line voltage. The developed PV-reinforced DVR system is designed with aid of a three-phase Voltage Source Converter (VSC), DC-link integrated with PV system and battery, and a coupling transformer. A controller based on Pulse Width Modulation (PWM) technique is designed to extract error voltage signal and generate gate pulses for the switches in the VSC.

2.1 DC-link design

The DC-link of the developed DVR is designed so as to provide voltage support at the Point of Common Coupling (PCC). The source voltage, V_s at the PCC is chosen to be 327V (as in the *(Farooqi, et al.*, 2022)). With the line-to-line voltage, V_{LL} obtained using the chosen V_s, (1) is used to calculate the magnitude of voltage at the DC-link,

$$V_{dc} = \frac{2\sqrt{2}}{\sqrt{3}} V_{LL} \quad (3.1)$$
$$= \frac{2\sqrt{2}}{\sqrt{3}} \times 327 \cong 534\text{V}$$

To match the DC-link voltage to the grid via the VSC, the DC-link capacitor rating is calculated using (2). The equation represents the energy storage capacity of DC-link chosen as 100kW.

$$E_s = \frac{1}{2} C_{dc} v_{r\_dc}^2 \quad (2)$$

Where v_{r_dc} is the rated DC-link voltage for the DVR converter chosen as 1.41kV, and C_{dc} is the capacitance of DC-link capacitor. This implies that

$$C_{dc} = \frac{2E_s}{v_{r\_dc}^2} \quad (3)$$
$$= \frac{2 \times 100 \times 10^3}{(1.41 \times 10^3)^2} = 0.1006F \cong 0.1F$$

Therefore, 100mF is chosen. A 100kW PV array is connected to the DC-link capacitor and the VSC, as shown in Figure 1.

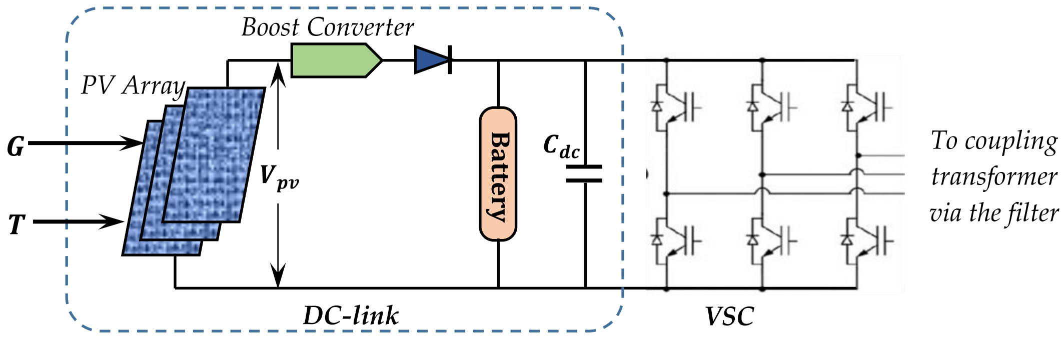

Figure 1: PV-reinforce DC-link configuration.

The PV array is connected to the battery and the DC-link capacitor via a boost converter to regulate PV voltage, V_{pv}. The AC output voltage of the VSC is then fed to the PCC via a filter and a coupling transformer. The coupling transformer maintains the voltage to the grid level and provides a galvanic isolation between the DC-link and the AC grid. Figure 2 shows the MATLAB/Simulink implementation of the DC-link of the developed DVR.

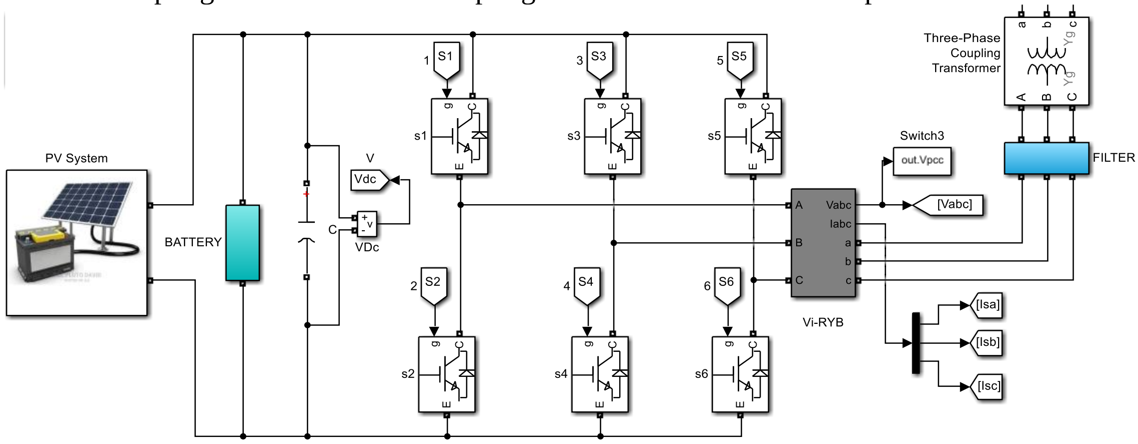

Figure 2: DC-link MATLAB/Simulink Model

Table 1 shows the parameters of the DC-link and that of the PV array.

Table 1: Parameters of DC-link and the PV array

Parameter	Values
No. Cell per module	72

Max. Power (W)/module	305kW
Open circuit voltage, V_{oc}	45.2V
Voltage at max. power point, V_{mppt}	35.6
Short Circuit current, I_{sc}	9A
Current at max. power point, I_{mppt}	8.6A
Capacitance of DC-link capacitor, C_{dc}	100*Mf*
DC-link rated voltage, V_{dc}	534V
source voltage, V_s	327V

2.2 DC-link voltage controller

The system always check for deviation in the voltage at the PCC. When the voltage deviates from the reference line voltage, V_{LL}, the DC-link capacitor releases voltage via the VSC. When the DC-link capacitor discharges below an SOC of 90%, the battery is used to support the voltage and at the same time charging the capacitor. When the battery is discharged below an SOC of 60%, the DC-link capacitor is recharged to 100% using the PV array. When the PV power is unavailable and the battery SOC is more than 20%, then the voltage support is provided using the battery. As such, the DC voltage is maintained. The flow chart for the DC-link voltage control is shown in Figure 3

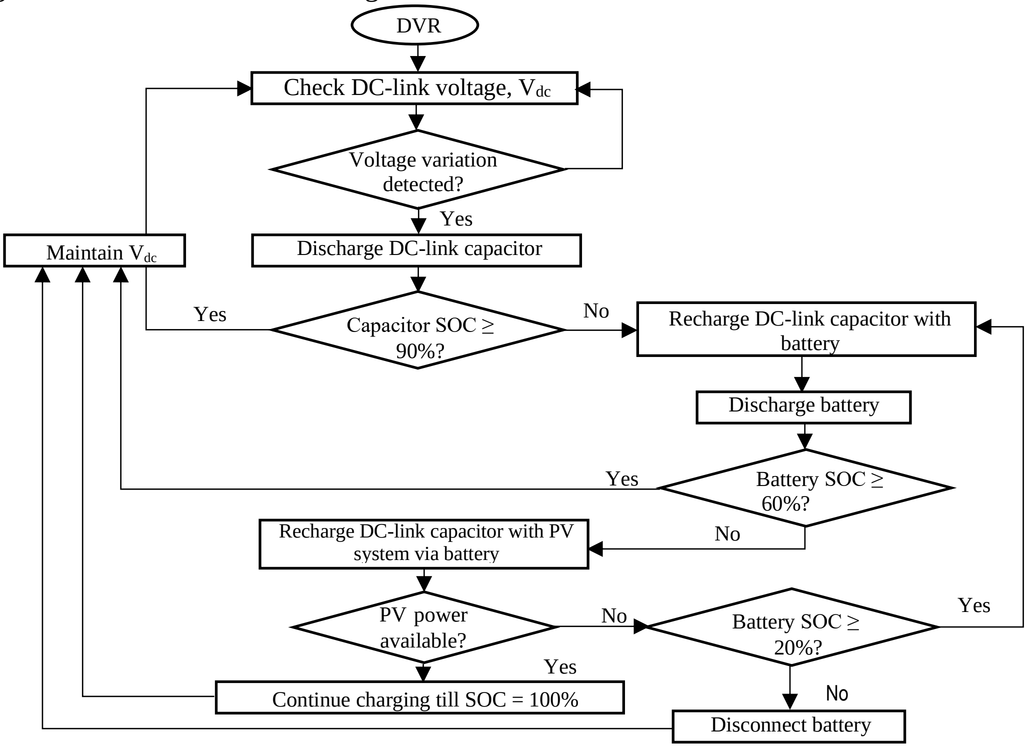

Figure 3: Flowchart of DC-link Voltage Control

Figure 4 presents the MATLAB/Simulink implementation of the DC-link voltage control developed.

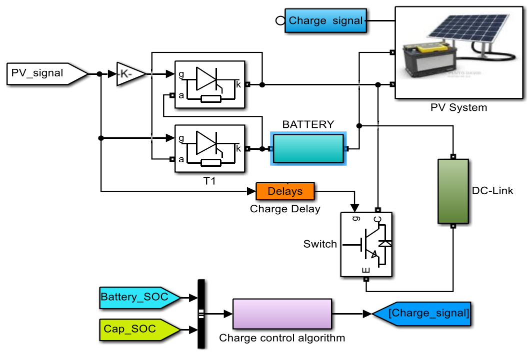

Figure 4: DC-link voltage control developed in MATLAB/Simulink

2.3 Voltage Source Converter (VSC) Design

The compensating voltage is injected by the DVR, V_{DVR} needs to be converted to AC since the power at PCC and the rest of the grid is AC form. A 3-arm, 6-pulse voltage source converter (VSC) is designed. A controller based on Pulse Width Modulation (PWM) technique is designed to extract error voltage signal and generate gate pulses for the MOSFETs in the VSC. A three phase reference voltage is generated according to equation (4)

From the reference voltage, a three-phase reference voltage is then generated using (5),

$$\begin{pmatrix} V_{a\_ref} \\ V_{b\_ref} \\ V_{c\_ref} \end{pmatrix} = V_{f\_ref} \begin{pmatrix} sin\omega t \\ sin\left(\omega t - \frac{2\pi}{3}\right) \\ sin\left(\omega t + \frac{2\pi}{3}\right) \end{pmatrix} \quad (5)$$

Subsequently, parks transformation method is used to detect imbalance voltages in the system as expressed in (6)

$$V_{f\_ref} = \sqrt{\frac{2}{3}} V_{LL} \quad (4)$$

$$\begin{pmatrix} V_d \\ V_q \\ V_0 \end{pmatrix} = \frac{2}{3} \begin{pmatrix} cos(\omega t) & cos\left(\omega t - \frac{2\pi}{3}\right) & cos\left(\omega t + \frac{2\pi}{3}\right) \\ -sin(\omega t) & -sin\left(\omega t - \frac{2\pi}{3}\right) & -sin\left(\omega t + \frac{2\pi}{3}\right) \\ \frac{1}{2} & \frac{1}{2} & \frac{1}{2} \end{pmatrix} \begin{pmatrix} V_a \\ V_b \\ V_c \end{pmatrix} \quad (6)$$

The imbalance voltage is then compared with reference voltage to generate an error signal, e_{dq0} as defined in (7)

$$|e_{dq0}| = \sqrt{\left(V_{ref\_d} - V_{L\_d}\right)^2 - \left(V_{ref\_q} - V_{L\_q}\right)^2 - \left(V_{ref\_0} - V_{L\_0}\right)^2} \quad (7)$$

The error signal is fed into first PI_1 controller that stabilizes the error gain as expressed in (8)

$$V_{c\_dq0} = K_{P1} e_{t\_dq0} + K_{I1} \int e_{t\_dq0} dt \quad (8)$$

$$V_{PI\_dq0} = V_{c\_dq0} - V_{s\_abc} \quad (9)$$

Figure 5 presents the MATLAB/Simulink implementation of the pulses generation of the VSC developed.

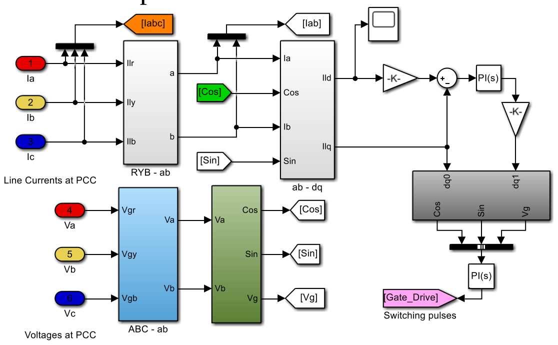

Figure 5: Switching pulses generation in MATLAB/Simulink

2.4 Coupling transformer

The coupling transformer steps up the voltage to the grid level and provides a galvanic isolation between the DC-link and the AC grid.

The equivalent model of the DVR is shown in figure 6 below

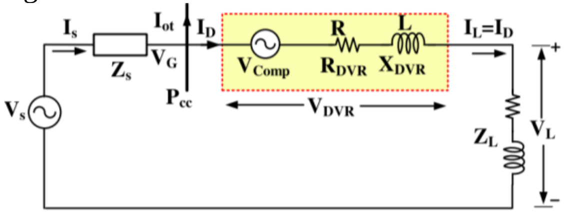

Figure 6: Equivalent Model of DVR

The voltage at PCC is represented by V_G and the voltage compensated by DVR is V_{DVR}. Resistance R and inductance L are obtained from the impedance Z of the filter and injection transformer

$$V_L(t) = V_G(t) + V_{DVR}(t) + Ri_L(t) + L\frac{d}{dt}i_L(t) \quad (10)$$

$$X_{DVR} = \frac{V_{DVR}^2}{S_{DVR}} X\ (pu) \quad (11)$$

$$R_{DVR} = \frac{V_{DVR}^2}{S_{DVR}} R\ (pu) \quad (12)$$

$$Z_{DVR} = \frac{V_{DVR}^2}{S_{DVR}} Z\ (pu) \quad (13)$$

When a voltage disturbance occurs within the DVR's operational range, the bypass switch immediately opens, the DVR enters active mode, and it supplies the grid with the necessary voltage. The bypass switch will close and the compensation mode will be terminated once the voltage returns to its usual range. In order to reduce the power loss in the DVR by limiting the adverse effect on line voltage, the DVR is momentarily withdrawn through a bypass switch because it is not essential to inject voltage into the grid under normal circumstances

To mitigate the harmonics injection by the PV system, an RC filter with R = 0.15Ω; and variable capacitor, C = 50 *m*F–250 *m*F is selected.

3. RESULTS AND DISCUSSION

The performance of the developed PV-DVR is ascertain by subjecting the system to three forms of faults; three-phase fault, Double Line-to-Ground (DLG) faults and Single Line-to-Ground fault.

3.1 Three-phase fault,

In the first scenario, the system is subjected to three phase symmetrical fault. Even though this type is not frequent due to its low probability of occurrence of 2 - 3%, however it has serious devastating impact. The fault is subjected within the time interval of $0.2sec \leq t_{sim} \leq 0.8sec$.

Due to the severe impact of the fault, the load voltage drop to 20.18V, which is 6.2% of the rated line voltage of 326.59V. Figure 7 and 8 show the source voltage and load voltage after the occurrence of the fault.

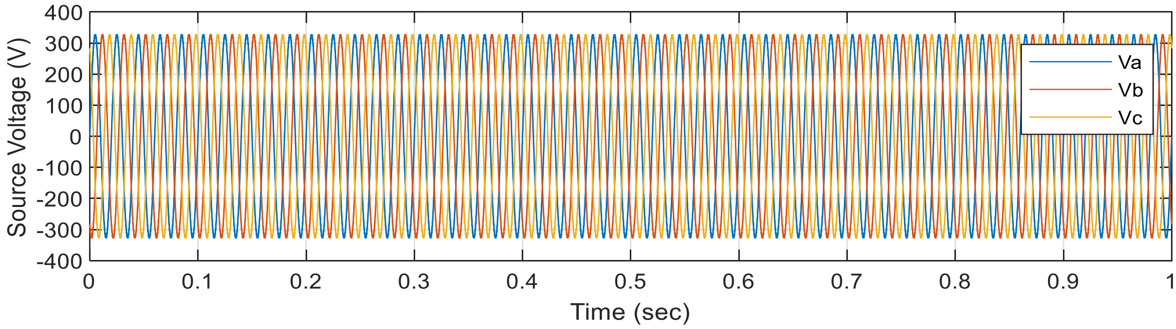

Figure 7: Source voltage

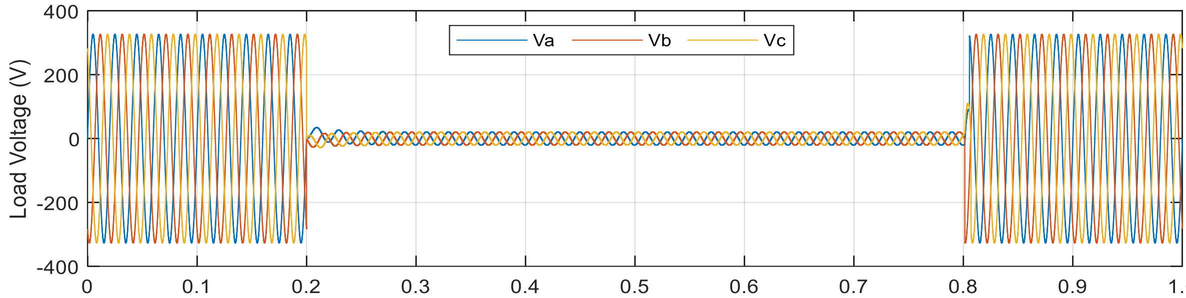

Figure 8: Load voltage after the occurrence of the three-phase fault

Having sensed the voltage deviation, the DVR injects a compensation voltage (shown in Figure 9) at the PCC. The DVR injected 278.06V to improve the faulted load voltage to 298.24V as shown in Figure 10.

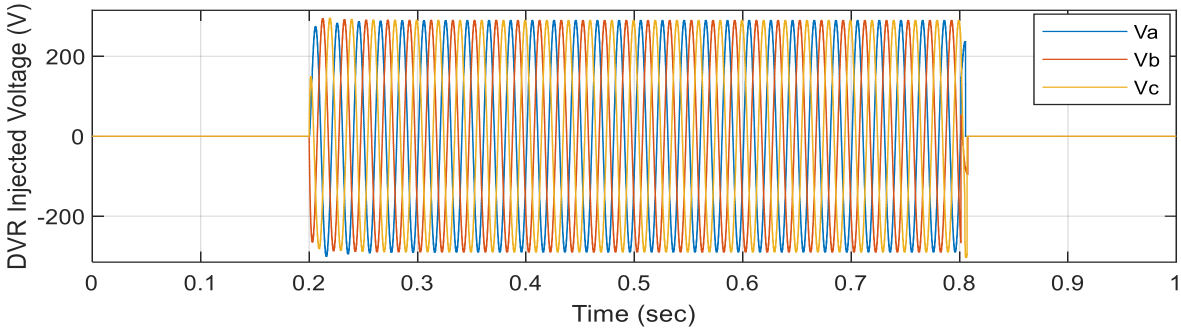

Figure 9: DVR compensating voltage after three fault without PV support

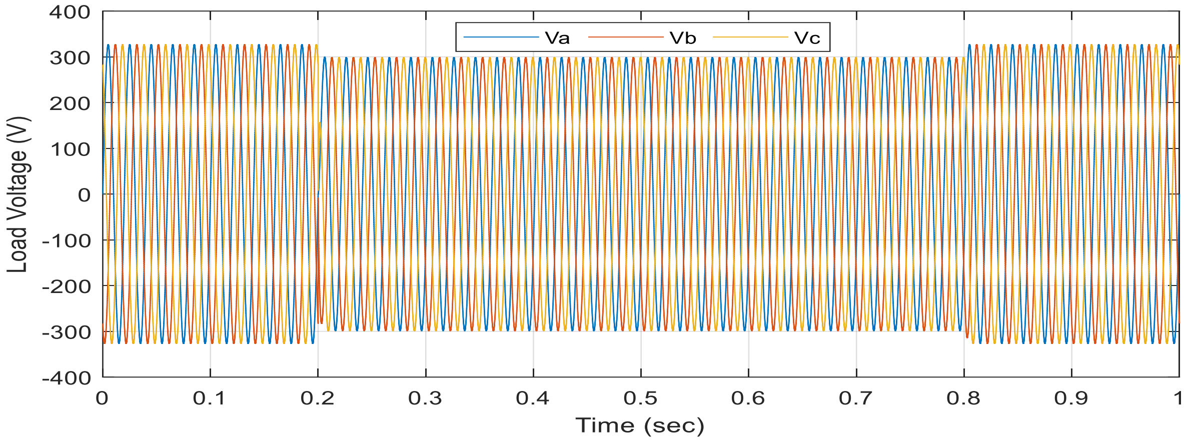

Figure 10: Load voltage after the three fault with DVR without PV support

Without the support of the PV-battery arrangement, the conventional DVR was able to boost the load voltage to 91.32% of the reference source voltage. This is in violation to the IEEE voltage requirement of $\pm 5\%$ of the nominal reference voltage. Table 2 summarized the voltage support of the DVR prior to the PV-reinforcement.

Table 2: Summary of DVR voltage support with three phase fault without the PV

Phase	**Source Voltage (V)**	**Load voltage (V)**		**% of V_{LOAD} to V_{SOURCE}**	**DVR Injected voltage (V)**
		Without DVR	**With DVR**		
A	326.59	20.18	298.24	91.32%	278.06
B	326.59	20.18	298.24	91.32%	278.06
C	326.59	20.18	298.24	91.32%	278.06

With the voltage support from the PV system, the PV-reinforced DVR injected a compensating voltage, V_{DVR} of 299.18V as shown in Figure 11. This boosted the load voltage from the 20.18V to 319.36V as shown in Figure 12.

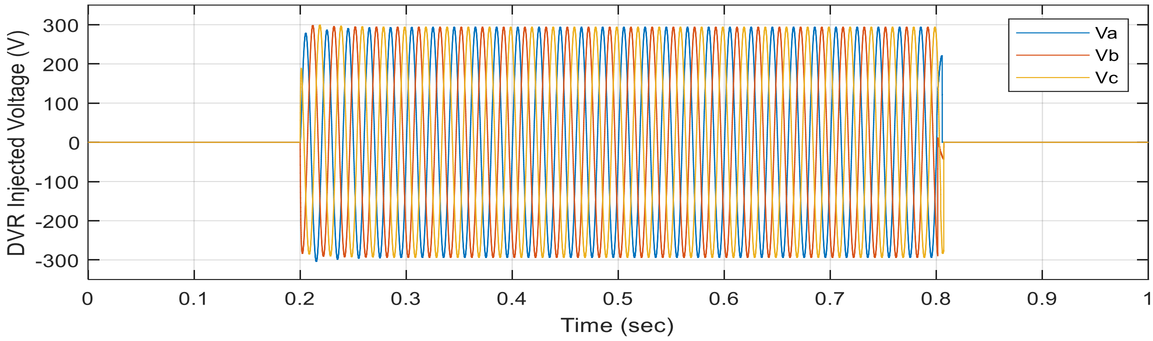

Figure 11: PV-reinforced DVR compensating voltage after three fault

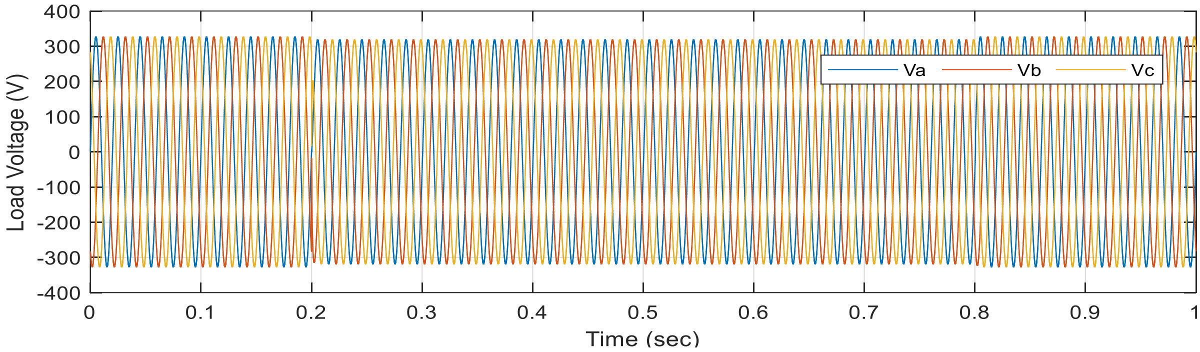

Figure 12: Load voltage after the three fault with DVR with PV support

Table 3: Summary of PV-reinforced DVR voltage support with three phase fault

Phase	Source Voltage (V)	Load voltage (V)		% of V_{LOAD} to V_{SOURCE}	Injected voltage, V_{PV_DVR} (V)
		Without DVR	PV-reinforced DVR		
A	326.59	20.18	319.36	97.79%	299.18
B	326.59	20.18	319.36	97.79%	299.18
C	326.59	20.18	319.36	97.79%	299.18

The PV-reinforced DVR was able to improve the voltage at PCC to 97.8% of the reference source voltage. It can be observed that the voltage has conform to the to the IEEE voltage requirement of ±5% of the nominal reference. Table 4.3 summarized the voltage support of the PV-reinforced DVRCompared to (Farooqi, et al., 2022), the PID-based DVR improved the load voltage to 300V in all the three phase when the three phase fault is subjected.

From the FFT analysis carried out, the load voltage Total Harmonic Distortion (THD_V) is found out to be 2.84%. Figure 13 shows the FFT analysis of the load voltage following the three phase fault.

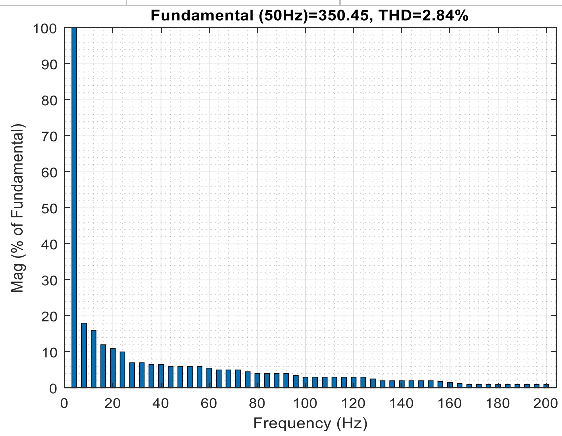

Figure 13: FFT analysis of the load voltage following the three phase fault.

Table 4 compares the load voltages and the THD_V obtained using the developed PV-reinforced DVR and that of PID-DVR presented in (Farooqi, et al., 2022)

Table 4: Comparative analysis for three phase fault scenario

Phase/ THD_V	**PID-DVR (Farooqi, et al., 2022)**	**Developed PV-reinforced DVR**	**% Improvement**
A	260.5	319.36	22.56%
B	260.5	319.36	22.56%
C	260.5	319.36	22.56%
THD_V	3.64%	2.84%	21.98%

From the comparative analysis, it can be seen that the PV-reinforced DVR performs better than the PID-DVR with voltage improvement capability of 22.56%

3.2 Double Line-to-Ground (DLG),
In the second scenario, the system is subjected to Double Line-to-Ground (DLG) unsymmetrical fault within the simulation time of $0.2sec \leq t_{sim} \leq 0.8sec$. This type of fault also has low probability of occurrence of less than 10%, however is more frequent than the three phase symmetrical fault.

Due to the occurrence of the fault, the load voltage on the faulted phases (B and C) drop to 126.40V, which is 38.7% of the rated line voltage, 326.59V. Figure 14 shows the load voltage after the occurrence of the DLG fault.

After detecting the voltage deviation in the phase B and C, the DVR injects a series compensation voltage (shown in Figure 15) at the PCC to improve the faulted phase load voltage to 295.68V and 292.25V respectively as shown in Figure 16.

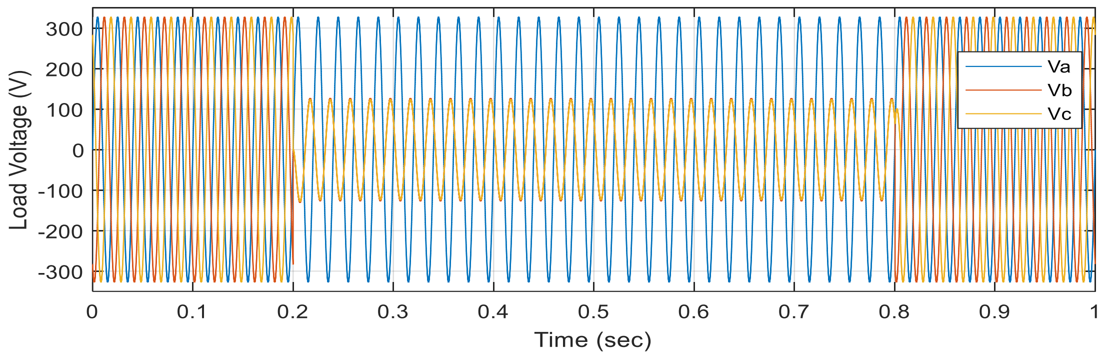

Figure 14: Load voltage after the DLG fault with DVR without PV support

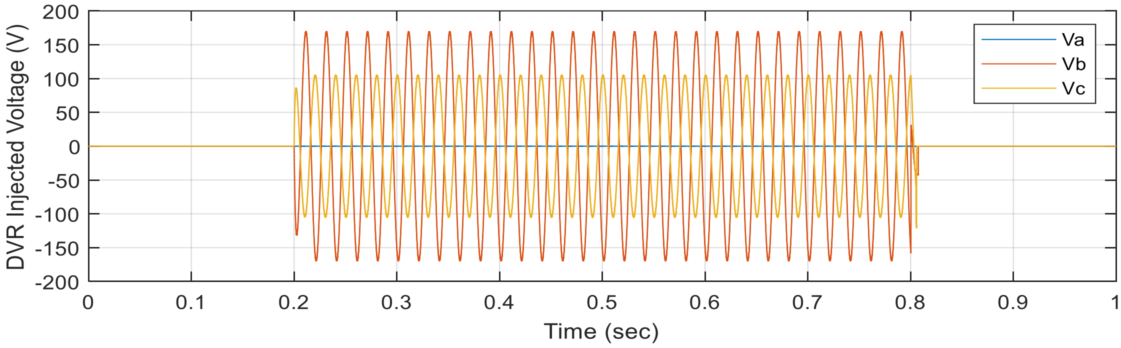

Figure 15: DVR compensating voltage after DLG fault without PV support

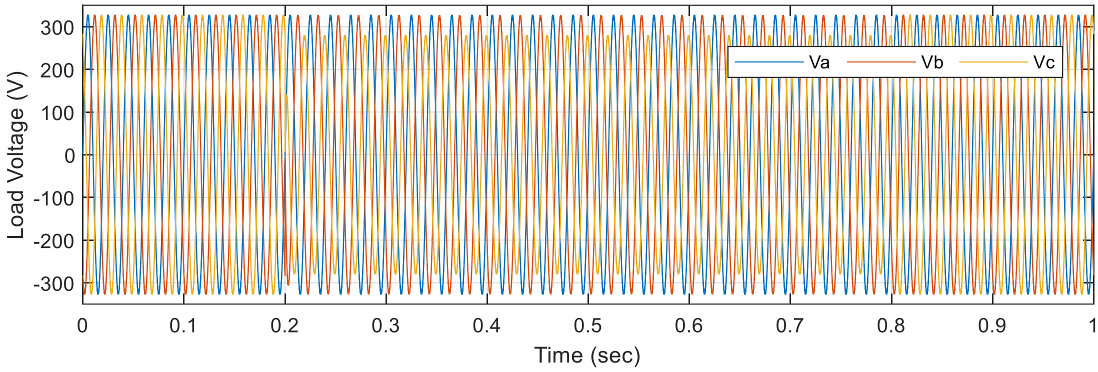

Figure 16: Load voltage after the DLG fault with DVR without PV support

Without the support of the PV-battery arrangement, the conventional DVR was able to boost the phase B and C load voltages to 90.54% and 89.49% of the reference source voltage respectively. These violated the IEEE voltage requirement of $\pm$5% of the nominal reference. Table 5 summarized the voltage support of the DVR prior to the PV-reinforcement.

Table 5: Summary of DVR voltage support with DLG fault without the PV

Phase	**Source Voltage (V)**	**Load voltage (V)**		**% of V_{LOAD} to V_{SOURCE}**	**DVR Injected voltage (V)**
		Without DVR	**With DVR**		
A	326.59	326.59	326.59	100%	0
B	326.59	126.40	295.68	90.54%	169.28
C	326.59	126.40	292.25	89.49%	165.85

With the voltage support from the PV system, the PV-reinforced DVR injected two phase compensating voltages shown in Figure 17 to boost the load voltages of the affected phases as shown in Figure 18.

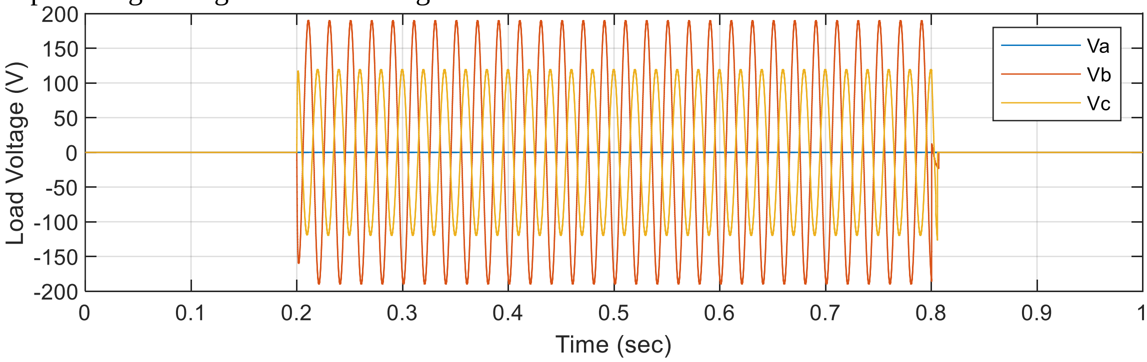

Figure 17: PV-reinforced DVR compensating voltage after the DLG fault

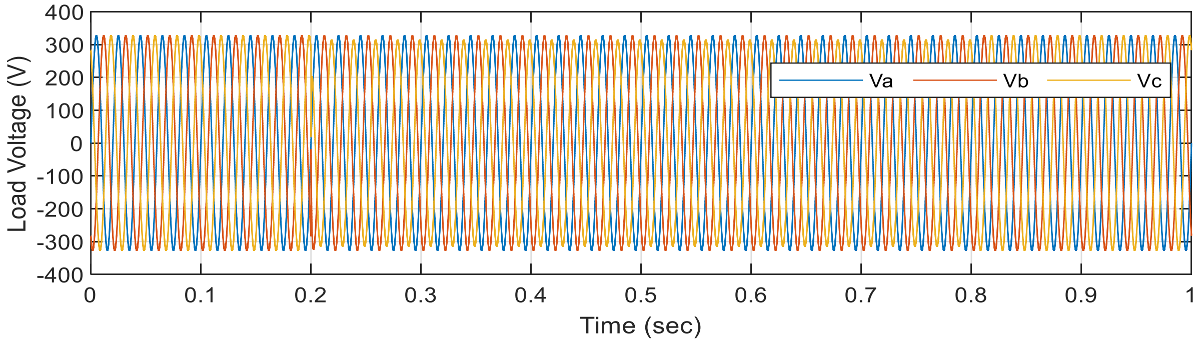

Figure 18: Load voltage after the DLG fault with PV-reinforced DVR

The PV-reinforced DVR was able to improve the voltage at PCC to 99.1% of the reference source voltage in both phases. It can be observed that the voltage has conform to the to the IEEE voltage requirement of ±5% of the nominal reference. Table 6 summarized the voltage support of the PV-reinforced DVR.

Table 6: Summary of PV-reinforced DVR voltage support with DLG fault

Phase	Source Voltage (V)	Load voltage (V)		% of V_{LOAD} to V_{SOURCE}	Injected voltage, V_{PV_DVR} (V)
		Without DVR	**PV-reinforced DVR**		
A	326.59	326.59	326.59	100%	0
B	326.59	126.40	323.66	99.1%	197.26
C	326.59	126.40	323.66	99.1%	197.26

Compared to (Farooqi, *et al.*, 2022), the PV reinforced DVR improved the load voltage to 323.66V in both phases as compared to 304V and 287V in the phase B and C respectively of the PID-DVR From the FFT analysis carried out, the load voltage Total Harmonic Distortion (THD_V) is found out to be 3.96%. Figure 19 shows the FFT analysis of the load voltage following the DLG fault.

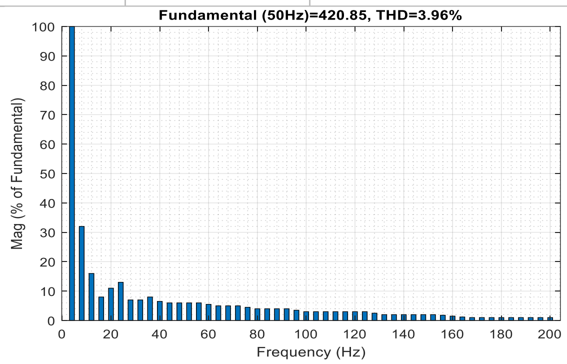

Figure 19: FFT analysis of the load voltage following the DLG fault.

Table 7 compares the load voltages and the THD_V obtained using the developed PV-reinforced DVR and that of PID-DVR presented in (Farooqi, *et al*., 2022)

Table 7: Comparative analysis for DLG fault scenario

Phase/ THD_V	**PID-DVR (Farooqi, et al., 2022)**	**Developed PV-reinforced DVR**	**% Improvement**
A	-	-	-
B	304	323.66	6.46%
C	287	323.66	12.77%
THD_V	5.10%	3.96%	22.35%

The comparative analysis shows an improvement of 6.4% and 12.77% on the voltages in Phase B and C of the developed DVR as compared to the PID-DVR. Also the THD was reduced to 3.96% from 5.10% which represents a 22.35% reduction

4. CONCLUSION

In this study, DC-link of conventional DVR is reinforced with Photovoltaic (PV) and battery with aim to moderate the devastating impact of symmetrical and unsymmetrical faults on the load voltage. Precisely, the PV-reinforced DVR is developed to mitigate voltage sags and harmonics caused by both symmetrical and unsymmetrical faults. The PV-reinforced DVR is designed to maintain a near-steady voltage at Point of Common Coupling (PCC). The developed DVR consists of a three-phase Voltage Source Converter (VSC), DC-link integrated with PV system and battery, and a coupling transformer. A controller based on Pulse Width Modulation (PWM) technique is designed to extract error voltage signal and generate gate pulses for the switches in the VSC. In order to mitigate the harmonics generated due to the injection of compensation voltage, a filter is designed to lessen the effect. To ascertain the performance of the developed PV-reinforced DVR, the system is designed in MATLAB/Simulink where a time-based simulation is carried out. From the simulation results obtained, it can be concluded that the load voltage levels and THD_V in all the scenarios are in conformity with the IEEE519 standards. It is observed that for the three phase fault, without the support of the PV-battery arrangement, the conventional DVR was able to boost the load voltage to 298.24V which is 91.32% of the reference source voltage. With the voltage support from the PV system, the PV-reinforced DVR injected 299.18V which boosted the load voltage from the 20.18V to 319.36V. Following the occurrence of the DLG fault, the load voltage on the faulted phases (B and C) drop to 126.40V, which is 38.7% of the rated source voltage, 326.59V. With the injection of series compensating voltages, the load voltages were improved to 99.1% of the rated source voltage. Furthermore, with aid of the designed filter, a significant reduction in the THD_V is obtained. Despite the improvement obtained, the PWM technique used for the generation of switching losses is characterized by high switching losses thereby impairing on the system efficiency. It is therefore recommended as further study to use better modulation techniques such as space vector modulation technique.

REFERENCES

Abdelkader, A. B., Mouloudi, Y., & Soumeur, M. A. (2022). Integration of renewable energy sources in the dynamic voltage restorer for improving power quality using ANFIS controller. Journal of King Saud University - Engineering Sciences, 34(8), 523-598..

Al-Mathnani, A. O., Lesewed, A., Ali, R. A., & Alsharef, A. A. (2021). Control of 48-Pulse Dynamic Voltage Restorer Using Tow Continuous Vector Controller. 2021 IEEE 1st International Maghreb Meeting of the Conference on Sciences and Techniques of Automatic Control and Computer Engineering MI-STA. Tripoli, Libya.

Berbaoui, & Brahim. (2017). Overview and investigation of the planned dynamic voltage restorer for autonomous electrical grid: Case of Adrar, south of Algeria. International Journal of Hydrogen Energy, 42(17), 12430-12447.

Boonchiam, P., & Mithulananthan, N. (2006). Dynamic Control Strategy in Medium Voltage DVR for Mitigating Voltage Sags/Swells. 2006 International Conference on Power System Technology. Chongqing, China.

Callegari, J. M., Cupertino, A. F., Ferreira, V. d., & Pereira, H. A. (2021). Minimum DC-Link Voltage Control for Efficiency and Reliability Improvement in PV Inverters. IEEE Transaction on Power Electronics, 36(5), 5512 - 5520.

Dehnavi, S. D., Negri, C., Bayne, S., & Giesselmann, M. (2022). Dynamic Voltage Restorer (DVR) with a novel robust control strategy. ISA Transactions, 121, 316-326.

Divyalakshmi, D., & Subramaniam, N. P. (2017). Photovoltaic based DVR with Power Quality Detection using Wavelet Transform. Energy Procedia, 117, 458-465.

Farooqi, A., Othman, M. M., Radzi, M. A., Musirin, I., Noor, S. Z., & Abidin, I. Z. (2022). Dynamic voltage restorer (DVR) enhancement in power quality mitigation with an adverse impact of unsymmetrical faults. *Energy Reports*, 8(1), 871-882.

Gambôa, P., Silva, J. F., Pinto, S. F., & Margato, E. (2019). Input–Output Linearization and PI controllers for AC–AC matrix converter based Dynamic Voltage Restorers with Flywheel Energy Storage: a Comparison. *Electric Power Systems Research*, 169, 214-228.

Gayatri, M. (2021). Power Quality Enhancement using Hybrid Energy Storage based Dynamic Voltage Restorer for Grid Integrated Distributed Generation. 2021 IEEE Bombay Section Signature Conference (IBSSC). Gwalior, India.

Guler, N., Bagheri, F., Bayhan, S., & Komurcugil, H. (2022). Single-Inductor Buck–Boost Inverter Based

Transformerless Dynamic Voltage Restorer. 2022 3rd International Conference on Smart Grid and Renewable Energy (SGRE). Doha, Qatar.

Hassanein, W. S., Ahmed, M. M., el-Raouf, M. O., Ashmawy, M. G., & Mosaad, M. I. (2020). Performance improvement of off-grid hybrid renewable energy system using dynamic voltage restorer. Alexandria Engineering Journal, 59(3), 1567-1581.

Mallick, N., & Mukherjee, V. (2020). Maximum power point tracking supported proton exchange membrane fuel cell based intelligent dynamic voltage restorer. International Journal of Hydrogen Energy, 45(53), 29271-29287.

Meloni, L. F., Rezek, Â. J., & Ribeiro, Ê. R. (2016). Small-signal modeling of a single-phase DVR for voltage sag mitigation. 2016 17th International Conference on Harmonics and Quality of Power (ICHQP). Belo Horizonte, Brazil.

Mishra, S. K., Bhuyan, S. K., & Rathod, P. V. (2022). Performance analysis of a hybrid renewable generation system connected to grid in the presence of DVR. Ain Shams Engineering Journal, 13(4), 101700.

Nicolaescu, G. I., Andrei, H., & Radulescu, S. (2015). Improvement of electricity distribution services using a DVR with a constant DC voltage source instaled in MV connection substations. 2015 IEEE 15th International Conference on Environment and Electrical Engineering (EEEIC). Rome, Italy.

Omar, A. I., Aleem, S. H., El-Zahab, E. E., Algablawy, M., & Ali, Z. M. (2019). An improved approach for robust control of dynamic voltage restorer and power quality enhancement using grasshopper optimization algorithm. ISA Transactions, 95, 110-129.

Omar, R., & Rahim, N. A. (2012). Voltage unbalanced compensation using dynamic voltage restorer based on supercapacitor. International Journal of Electrical Power & Energy Systems, 43(1), 573-581.

Pandya, R., & Bhavsar, F. (2018). Study on Compensation of Voltage Sag and Voltage Swell by Using DVR (Dynamic Voltage Restorer). 2018 International Conference on Current Trends towards Converging Technologies (ICCTCT). Coimbatore, India.

Prasad, M., & Akella, A. K. (2018). Voltage and Current Quality Improvement by Solar Photovoltaic fed ZSI-DVR. Procedia Computer Science, 125, 434-441.

Ramasamy, M., & Thangavel, S. (2011). Photovoltaic Based Dynamic Voltage Restorer with Outage Handling Capability Using PI Controller. Energy Procedia, 12, 560-569.

Ramasamy, M., & Thangavel, S. (2013). Experimental verification of PV based Dynamic Voltage Restorer (PV-DVR) with significant energy conservation. International Journal of Electrical Power & Energy Systems, 49, 296-307.

Rao, N. S., (2015). Simulation of Artificial Intelligent Controller Based DVR for Power Quality Improvement. Procedia Computer Science, 47, 153-167.

Rao, N. S., Priyadharson, A. S., & Dr., J. P. (2015). Simulation of Artificial Intelligent Controller Based DVR for Power Quality Improvement. Procedia Computer Science, 47, 153-167.

Sadigh, A. K., & Smedley, K. M. (2016). Fast and precise voltage sag detection method for dynamic voltage restorer (DVR) application. Electric Power Systems Research, 130, 192-207.

Saveca, J., Wang, Z., & Sun, Y. (2019). Dynamic Voltage Restorer-based Quality Optimization using Differential Evolution Algorithm. Elsevier, 2nd International Conference on Sustainable Materials Processing and Manufacturing, IEEE.

Seershak, M., & Ramees, K. M. (2022). Power Quality Improvement Using ZSI-DVR. 2022 International Conference on Futuristic Technologies in Control Systems & Renewable Energy (ICFCR). Malappuram, India.

Shady, A. I., Aleem, H. E., El-Zahab, E. E., Algablawy, M., & Ali, Z. M. (2019). An improved approach for robust control of dynamic voltage restorer and power quality enhancement using grasshopper optimization algorithm. ISA Transactions, 95, 110-129.

Shakir, & Sharma, M. (2019). IRPT Based DVR Application for Voltage Enhancement. 2019 6th International Conference on Signal Processing and Integrated Networks (SPIN). Noida, India.

Shuai, Z., Yao, P., Z., J. S., Tu, C., Jiang, F., & Cheng, Y. (2015). Design Considerations of a Fault Current Limiting Dynamic Voltage Restorer (FCL-DVR). IEEE Transactions on Smart Grid, 6(1), 14 - 25.